Electronic Supplementary Material (ESI) for Physical Chemistry Chemical Physics.

Electronic Supplementary Information

Photodissociation of $C_2F_4I_2$ in solid *para*-hydrogen: infrared spectrum of *anti-* and *gauche-*•C_2F_4I radicals

Karolina A. Haupa[a], Manho Lim[b], and Yuan-Pern Lee[a,c,d]

[a] *Department of Applied Chemistry and Institute of Molecular Science, National Chiao Tung University, Hsinchu 30010, Taiwan, E-mail: (KAH) karolina.haupa@gmail.com (YPL) yplee@mail.nctu.edu.tw, Tel: +886-3-5131459*

[b] *Department of Chemistry and Chemistry Institute for Functional Materials, Pusan National University, Busan 46241, Korea, E-mail: (ML) mhlim@pusan.ac.kr, Tel:* +82-51-510-2243

[c] *Institute of Atomic and Molecular Sciences, Academia Sinica, Taipei 10617, Taiwan.*

[d] Center for Emergent Functional Matter Science, National Chiao Tung University, Hsinchu 30010, Taiwan.

Tables and Figures in the ESI:

Comparisons of observed vibrational wavenumbers and IR intensities of *anti-* and *gauche*-CF_2ICF_2I with those calculated with the B3PW91/aug-cc-pVTZ-pp method are presented in Tables S1 and S2, respectively. Vibrational wavenumbers and IR intensities of *bridged*-C_2F_4I calculated with the B3PW91/aug-cc-pVTZ-pp method are presented in Table S3. Mixing ratios (in ppm) of *anti*-CF_2ICF_2I, *gauche*-CF_2ICF_2I, *anti*-•C_2F_4I, *gauche*-•C_2F_4I, and C_2F_4 at various stages of different experiments are listed in Table S4. The vertical excitation energies and oscillator strengths of *anti*-CF_2ICF_2I, *gauche*-CF_2ICF_2I, *anti*-•C_2F_4I, and *gauche*-•C_2F_4I calculated with the CAM-B3LYP/aug-cc-pVTZ-pp method are presented in Table S5.

Geometries of *anti-* and *gauche*-CF_2ICF_2I conformers optimized with the B3PW91/aug-cc-pVTZ-pp method are presented in Fig. S1. Relaxed energy profiles for the internal rotation of CF_2ICF_2I calculated with the B3PW91/aug-cc-pVTZ-pp method is presented in Fig. S2. Linear fit of experimental wavenumbers versus harmonic vibrational wavenumbers of CF_2ICF_2I calculated with the B3PW91/aug-cc-pVTZ-pp method is presented in Fig. S3. Normalized partial difference spectra of a matrix $CF_2ICF_2I/p\text{-}H_2$ in the range 1350–1230 cm^{-1} recorded after irradiation of the matrix with light near 300, 280, and 265 nm are presented in Fig. S4.

Table S1 Comparison of observed vibrational wavenumbers and IR intensities of *anti*-CF_2ICF_2I (C_{2h}) with those calculated with the B3PW91/aug-cc-pVTZ-pp method

Mode[a]	Sym.	*p*-H_2		Solution[c,d]	Harmonic[e]			Anharmonic		PED (%)[f,g]
		ν /cm^{-1}	Int.[b]	ν /cm^{-1}	ν^{sc} /cm^{-1}	ν /cm^{-1}	Int. /km mol^{-1}	ν /cm^{-1}	Int. /km mol^{-1}	
ν_1	A_g				1224	1237	0	1217	0	$-\nu F_1C_1 (11) - \nu F_2C_1 (11) - \nu F_3C_2 (11) - \nu F_4C_2 (11) + \nu C_1C_2 (37)$
ν_2	A_u	1167.0	30	1159[b]/1169[c]	1176	1188	257	1168	250	$-\nu F_1C_1 (25) + \nu F_2C_1 (25) - \nu F_3C_1 (25) + \nu F_4C_2 (25)$
ν_3	B_g				1166	1178	0	1156	0	$-\nu F_1C_1 (19) + \nu F_2C_1 (19) + \nu F_3C_2 (19) - \nu F_4C_2 (19)$
ν_4	B_u	1116.7	31	1109[b]/1116[c]	1125	1135	316	1123	311	$-\nu F_1C_1 (21) - \nu F_2C_1 (21) + \nu F_3C_2 (21) + \nu F_4C_2 (21)$
ν_5	A_g			995–997[b]	965	971	0	958	0	$-\nu C_1C_2 (17) + \delta F_2C_1F_1 (20) + \delta F_4C_2F_4 (20)$
ν_6	B_u	707.8 /709.6	100	709[b]/709[c]	704	702	386	697	372	$-\nu I_1C_1 (14) + \nu I_2C_2 (14) + \delta I_1C_1C_2 (24) - \delta I_2C_2C_1 (24)$
ν_7	A_g			670[b]	683	681	0	681	0	$\nu C_1C_2 (11) + \delta F_2C_1F_1 (12) + \delta F_2C_1F_4 (12)$
ν_8	B_u	574.9	1	575[b]/584[c]	585	580	4	579	4	$-\delta F_2C_1F_1 (37) + \delta F_4C_2F_3 (37)$
ν_9	B_g				524	517	0	515	0	$-\gamma F_3C_1I_2C_2 (32) + \gamma F_1C_2I_1C_1 (32)$
ν_{10}	A_g				373	362	0	361	0	$-\nu C_1C_2 (25) + \delta F_2C_1F_1 (31) + \delta F_4C_2F_3 (31)$
ν_{11}	A_u				299	286	0	285	0	$-\nu I_1C_1 (35) + \nu I_2C_2 (35) - \delta I_1C_1C_2 (10) + \delta I_2C_2C_1 (10)$
ν_{12}	B_g				297	284	0	281	0	$\delta F_1C_1I_1 (33) + \delta F_3C_2I_2 (33)$
ν_{13}	A_g			268[b]	281	268	0	266	0	$\nu I_1C_1 (24) + \nu I_2C_2 (24) - \delta I_1C_1C_2 (13) - \delta I_2C_2C_1 (13)$
ν_{14}	B_g				270	257	0	253	0	$-\delta F_1C_1I_1 (42) + \delta F_3C_2I_2 (42)$
ν_{15}	A_u				231	216	0	211	0	$-\gamma F_3C_1I_2C_2 (37) - \gamma F_1C_2I_1C_1 (37)$
ν_{16}	A_g			133[b]	148	131	0	130	0	$-\nu I_1C_1 (20) - \nu I_2C_2 (20) - \delta I_1C_1C_2 (26) - \delta I_2C_2C_2 (26)$
ν_{17}	B_u				119	101	1	101	1	$-\delta I_1C_1C_2 (46) + \delta I_2C_2C_1 (46)$
ν_{18}	A_u				70	50	0	43	0	$\tau I_2C_2C_1I_1 (96)$

[a] For ease of comparison with the other isomers, mode numbers are ordered according to vibrational wavenumbers instead of symmetry. [b] Percentage IR intensities relative to the most intense line (ν_6). [c] In methanol. M. T. Messina, P. Metrangolo, W. Navarrini, S. Radice, G. Resnati, and G. Zerbi, *J. Mol. Struct.* **2000**, *524*, 87. [d] In methanol. J. Liang, D. Drake, and M. Roselius, *Appl. Sepctrosc.* **1994**, *48*, 206. [e] ν^{sc} : scaled harmonic vibrational wavenumber, with linear scaling factor: 0.9725*x* + 20.6; see text. [f] Terms with percentage coefficient >10 % are included; the percentage coefficients are listed in parentheses. [g] Mode description: ν: stretch, δ: bend, γ: out-of-plane deformation, τ: torsion. Atomic numbering is indicated in Fig. S1.

Table S2 Comparison of observed vibrational wavenumbers and IR intensities of *gauche*-CF_2ICF_2I (C_2) with those calculated with the B3PW91/aug-cc-pVTZ-pp method

Mode[a]	Sym.	p-H_2		Solution[c,d]	Harmonic[e]			Anharmonic		PED (%)[f,g]
		ν /cm^{-1}	Int.[b]	ν /cm^{-1}	ν^{sc} /cm^{-1}	ν /cm^{-1}	Int. /km mol^{-1}	ν /cm^{-1}	Int. /km mol^{-1}	
ν_1	A	1216.1	89	1207[b]/1215[c]	1204	1217	231	1188	214	$-\nu F_1C_1 (13) - \nu F_3C_2 (13) - \nu F_2C_1 (12) - \nu F_4C_2 (12) + \nu C_1C_2 (31)$
ν_2	B	1154.1	94		1159	1171	246	1143	231	$-\nu F_1C_1 (40) + \nu F_3C_2 (40)$
ν_3	A	1144.4	15		1147	1158	55	1129	49	$-\nu F_1C_1 (19) - \nu F_3C_2 (19) + \nu F_2C_1 (22) + \nu F_4C_2 (22)$
ν_4	B	1083.0	16		1084	1094	35	1067	31	$-\nu F_2C_1 (34) + \nu F_4C_2 (34)$
ν_5	A	983.7	16	974[b]/982[c]	970	976	247	958	239	$-\nu F_2C_1 (11) - \nu F_4C_2 (11) - \nu C_1C_2 (31)$
ν_6	B	841.3	100	835[b]/841[c]	836	838	248	827	249	$-\gamma F_4C_1F_3C_2 (34) - \gamma F_2C_2F_2C_1 (34)$
ν_7	A	636.8	4		647	645	11	638	11	$-\nu F_1C_1 (11) - \nu F_3C_2 (11) - \delta F_2C_1F_1 (25) - \delta F_3C_2F_4 (25)$
ν_8	B	583.2	1		593	589	15	584	14	$-\delta F_2C_1F_1 (32) + \delta F_3C_2F_4 (32)$
ν_9	A				458	450	1	444	1	$-\gamma F_3C_1I_2C_2 (28) + \gamma F_1C_2I_1C_1 (28)$
ν_{10}	A				342	331	1	326	1	$-\delta F_2C_1F_1 (11) + \delta F_3C_2F_4 (11) + \gamma F_3C_1I_2C_2 (28) - \gamma F_1C_2I_1C_1 (28)$
ν_{11}	A				313	301	2	298	2	$-\nu C_1C_2 (14) - \nu C_1C_2 (34) + \nu C_1I_1 (34)$
ν_{12}	B				296	283	0	279	0	$\nu C_1C_2 (31) + \nu C_1I_1 (31) + \nu C_2I_2 (31)$
ν_{13}	B				292	279	0	276	0	$\nu C_1C_2 (11) + \nu C_1C_2 (23) + \nu C_1I_1 (23)$
ν_{14}	A				263	249	0	247	0	$\nu C_1C_2 (19) - \nu C_1I_1 (19) + \delta F_1C_1I_1 (27) + \delta F_3C_2I_2 (27)$
ν_{15}	B				254	240	1	237	1	$\nu C_1C_2 (21) - \nu C_1I_1 (21) - \delta F_1C_1I_1 (14) + \delta F_3C_2I_2 (14) + \gamma F_3C_1F_7C_2 (28) - \gamma F_1C_2F_1C_1 (28)$
ν_{16}	B				172	156	1	153	1	$-\delta I_1C_1C_2 (29) + \delta I_2C_2C_1 (29) - \gamma F_3C_1I_2C_2 (14) + \gamma F_1C_2I_1C_1 (14)$
ν_{17}	A				108	90	0	87	0	$\delta I_1C_1C_2 (41) + \delta I_2C_2C_1 (41)$
ν_{18}	A				71	52	0	46	0	$\tau I_2C_2C_1I_1 (94)$

[a] For ease of comparison with the other isomers, mode numbers are ordered according to vibrational wavenumbers instead of symmetry. [b] Percentage IR intensities relative to the most intense line (ν_6). [c] In methanol. M. T. Messina, P. Metrangolo, W. Navarrini, S. Radice, G. Resnati, and G. Zerbi, *J. Mol. Struct.* **2000**, *524*, 87. [d] In methanol. J. Liang, D. Drake, and M. Roselius, *Appl. Sepctrosc.* **1994**, *48*, 206. [e] ν^{sc} : scaled harmonic vibrational wavenumber, with linear scaling factor: $0.9725x + 20.6$; see text. [f] Terms with percentage coefficient >10 % are included; the coefficients are listed in parentheses. [g] Mode description: ν: stretch, δ: bend, γ: out-of-plane deformation, τ: torsion. Atomic numbering is indicated in Fig. S1.

Table S3 Vibrational wavenumbers and IR intensities of *bridged*-C_2F_4I (C_{2v}) calculated with the B3PW91/aug-cc-pVTZ-pp method.

Mode[a]	Symmetry	Harmonic[b]			Anharmonic	
		ν /cm^{-1}	ν^{sc} /cm^{-1}	Int. /km mol^{-1}	ν /cm^{-1}	Int. /km mol^{-1}
ν_1	A_1	1772	1744	810	1726	730
ν_2	A_2	1390	1373	0	1365	0
ν_3	B_1	1384	1367	360	1354	351
ν_4	B_2	1213	1200	322	1193	317
ν_5	A_1	809	808	19	792	14
ν_6	B_2	569	574	3	564	3
ν_7	A_2	552	558	0	544	0
ν_8	B_2	461	469	10	431	7
ν_9	A_1	449	457	3	440	3
ν_{10}	A_1	393	403	3	388	2
ν_{11}	B_1	214	229	3	212	3
ν_{12}	A_2	200	215	0	194	0
ν_{13}	B_1	86	104	0	79	0
ν_{14}	A_1	78	97	1	73	1
ν_{15}	B_2	57	76	0	46	0

[a] For ease of comparison with the other isomers, mode numbers are ordered according to vibrational wavenumbers instead of symmetry. [b] ν^{sc} : scaled harmonic vibrational wavenumber, with linear scaling factor: $0.9725x + 20.6$; see text.

Table S4 Mixing ratios (in ppm) of *anti*-CF_2ICF_2I, *gauche*-CF_2ICF_2I, *anti*-$\bullet C_2F_4I$, *gauche*-$\bullet C_2F_4I$, and C_2F_4 at various stages in experiments I–V.

Expt.	Stage	*anti*-CF_2ICF_2I	*gauche*-CF_2ICF_2I	*anti*-$\bullet C_2F_4I$	*gauche*-$\bullet C_2F_4I$	C_2F_4
I	Deposition (4 h)	5.90	1.01	0.00	0.00	0.00
	Irradiation (300 nm, LED, 2 h)	5.30 (−0.60)	0.99 (−0.02)	0.43	0.22	0.17
	Irradiation (300 nm, LED, 4 h)	4.84 (−1.06)	0.98 (−0.03)	0.61	0.36	0.33
II	Deposition (4.5 h)	15.50	3.77	0.00	0.00	0.00
	Irradiation (280 nm, LED, 2h)	14.44 (−1.06)	3.68 (−0.09)	1.45	0.85	0.56
	Irradiation (280 nm, LED, 4 h)	14.20 (−1.30)	3.62 (−0.15)	1.88	1.21	0.79
II	Deposition (4 h)	12.63	2.60	0.00	0.00	0.00
	Irradiation (265 nm, LED, 2 h)	12.39 (−0.24)	2.52 (−0.08)	0.13	0.21	0.23
	Irradiation (265 nm, LED, 4 h)	12.13 (−0.50)	2.47 (−0.13)	0.26	0.51	0.40
IV	Deposition (5 h)	15.11	3.56	0.00	0.00	0.00
	Irradiation (281 nm, Laser, 3 min)	11.51 (−3.60)	3.06 (−0.50)	2.53	2.95	1.88
	Irradiation (267 nm, Laser, 3 min)	11.01 (−0.50)	2.94 (−0.12)	2.39 (−0.14)	3.34 (+0.39)	3.27 (+1.39)
V	Deposition (5 h)	11.90	2.39	0.00	0.00	0.00
	Irradiation (280 nm, LED, 2h)	9.88 (−2.02)	2.26 (−0.13)	1.73	1.11	0.81
	Irradiation (265 nm, LED, 2h)	9.74 (−0.14)	2.23 (−0.03)	1.70 (−0.03)	1.18 (+0.07)	0.94 (+0.13)
	Irradiation (300 nm, LED, 2h)	7.32 (−2.42)	2.14 (−0.09)	2.37 (+0.67)	1.88 (+0.70)	2.47 (+1.53)
	Irradiation (365 nm, LED, 20 min)	7.18 (−0.14)	2.13 (−0.01)	1.28 (−1.09)	1.89 (+0.01)	3.51 (+1.04)

[a] All experiments were performed on matrices with CF_2ICF_2I /*p*-H_2 = ~1/20 000. The smaller mixing ratio of the precursor in Experiment I is because of the lack of passivation.

Table S5 Vertical excitation energies (Δ*E*) and oscillator strengths (*f*) of the first eight singlet transitions of *anti*-CF_2ICF_2I, *gauche*-CF_2ICF_2I, *anti*-$\bullet C_2F_4I$ and *gauche*-$\bullet C_2F_4I$ calculated with the CAM-B3LYP/aug-cc-pVTZ-pp method at the B3PW91/aug-cc-pVTZ-pp optimized geometry.

Transition	*anti*-CF_2ICF_2I		*gauche*-CF_2ICF_2I		*anti*-$\bullet C_2F_4I$		*gauche*-$\bullet C_2F_4I$	
	Δ*E* /nm	*f* /10^{-3}	Δ*E* /nm	*f* /10^{-3}	Δ*E* /nm	*f* /10^{-3}	Δ*E* /nm	*f* /10^{-3}
$S_0 \rightarrow S_1$	285	4.0	275	0.9	388	0.0	320	0.0
$S_1 \rightarrow S_2$	283	0.0	269	0.1	382	0.7	317	0.0
$S_2 \rightarrow S_3$	278	0.0	267	0.0	294	26.6	274	1.2
$S_3 \rightarrow S_4$	273	0.0	265	0.0	276	0.0	267	0.1
$S_4 \rightarrow S_5$	189	0.0	201	4.2	272	0.0	253	5.7
$S_5 \rightarrow S_6$	189	605.6	200	0.7	227	180.6	251	1.6
$S_6 \rightarrow S_7$	188	0.0	199	2.0	213	0.3	249	4.2
$S_7 \rightarrow S_8$	186	0.4	196	11.4	210	56.1	232	0.1

(a) *anti*-CF_2ICF_2I

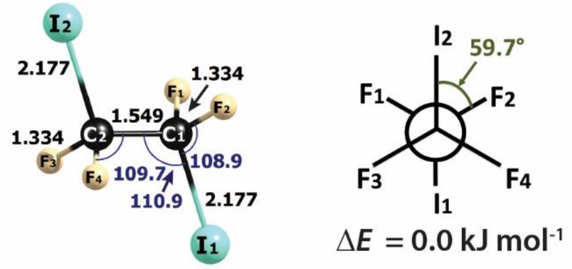

(b) *gauche*-CF_2ICF_2I

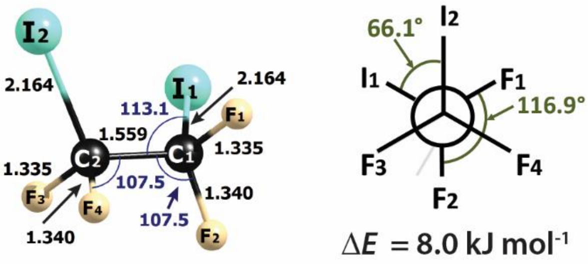

Fig. S1 Geometries of CF_2ICF_2I conformers: (a) *anti*-CF_2ICF_2I and (b) *gauche*-CF_2ICF_2I . The structures were optimized with the B3PW91/aug-cc-pVTZ-pp method; bond lengths are in Å and angles in degree.

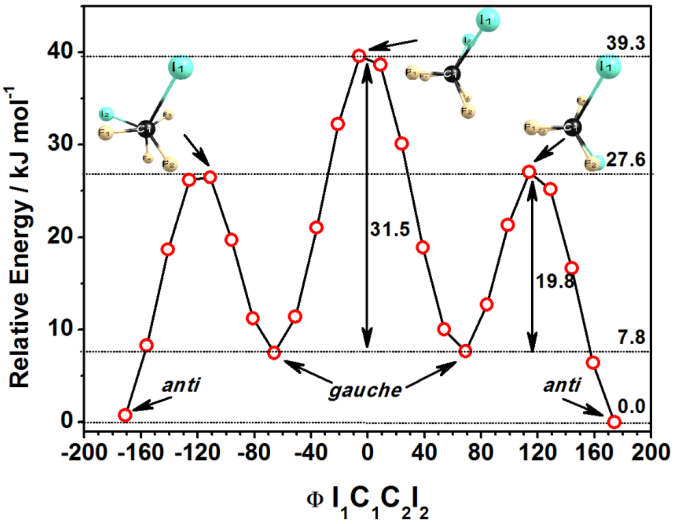

Fig. S2 Relaxed energy profiles for the internal rotation ($\Phi I_1C_1C_2I_2$) of CF_2ICF_2I calculated with the B3PW91/aug-cc-pVTZ-pp method; the open circles denote energies of the optimized structures.

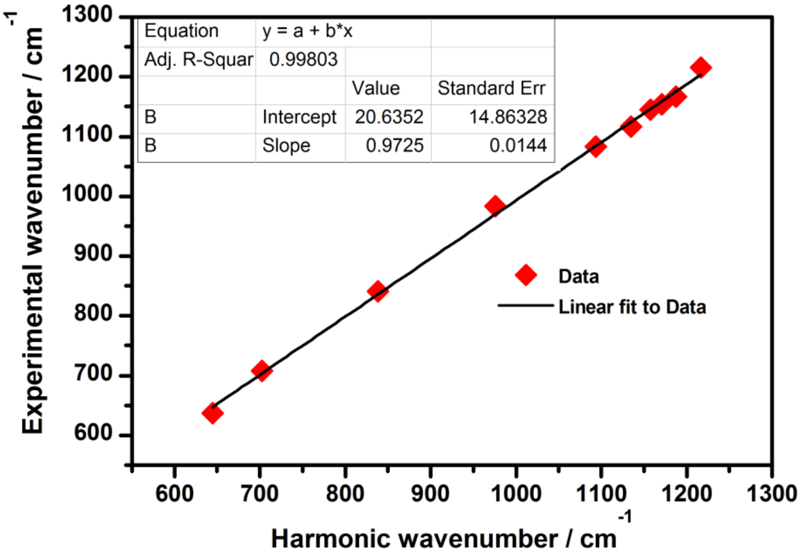

Fig. S3 Linear fit of experimental wavenumbers versus harmonic vibrational wavenumbers of CF_2ICF_2I calculated with the B3PW91/aug-cc-pVTZ-pp method. The data corresponding to both isomers were used.

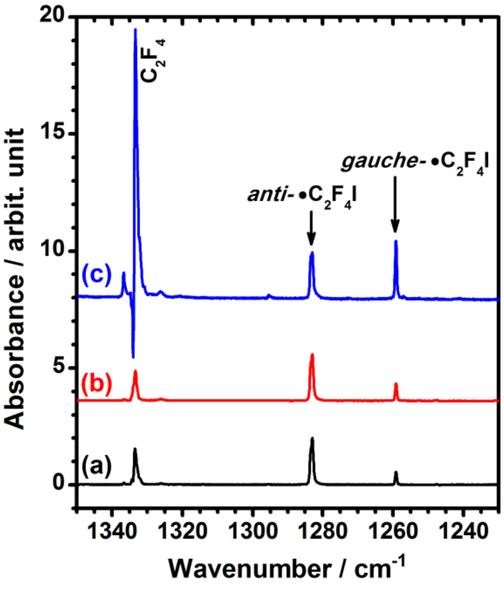

Fig. S4 Partial difference spectra of a matrix CF_2ICF_2I/*p*-H_2 (~1/20 000) in the range 1350-1230 cm^{-1} recorded after irradiation of the matrix with light near 300 nm for 3 h (a), 280 nm for 3 h (b), and 265 nm for 3 h (c). The spectra were normalized to the line of *anti*-•C_2F_4I near 1285 cm^{-1}. Lines of *anti*- and *gauche*-•C_2F_4I are marked with arrows and labels.